Lasers in Manufacturing Conference 2025

Selective element evaporation via laser de-alloying to improve the formability of high-strength aluminium alloy 7075

Marcel Stephan[a, b], Dominic Neumayer[a], Lova Chechik[b, c], Dominic Bartels[a, b, c], Stephan Roth[a, b], Michael Schmidt[b, c]

[a]*Bayerisches Laserzentrum gemeinnützige Forschungsgesellschaft mbH (BLZ), Konrad-Zus-Straße 2-6, 91052 Erlangen, Germany*
[b]*Friedrich-Alexander-Universität Erlangen-Nürnberg (FAU), Erlangen Graduate School in Advanced Optical Technologies (SAOT), Paul-Gordan-Str. 6, 91052 Erlangen, Germany*
[c]*Friedrich-Alexander-Universität (FAU), Institute of Photonic Technologies (LPT), Konrad-Zuse-Straße 3-5, 91052 Erlangen, Germany*

Abstract

Aluminium alloys of the 7xxx series are renowned for their exceptional strength due to Mg and Zn precipitations. However, the presence of these precipitations reduces the ductility and thus the formability of these alloys, hindering their application for shaping operations e.g. in the automotive sector. One promising approach to improve the formability of this material class is by selectively evaporating these precipitation-promoting elements exploiting their lower evaporation temperature compared to the aluminium matrix. A spatially resolved evaporation can be achieved by localised laser remelting.

In this work, we present results on the selective element evaporation for AA7075. Key characteristics for describing the process are the evaporated amount of elements, the evaporation depth and gradients along z-direction. Cross-sections are analysed using EDX to determine the elemental distribution. Finally, element evaporation is correlated with melt pool size and the applied processing strategy to assess the potentials of a specific laser process
Keywords: Laser welding; Aluminium; Hybrid manufacturing

1. Introduction

Aluminium alloys are compelling materials for various industries, especially due to their high specific strength. Ternary 6xxx (Al-Mg-Si) series wrought alloys, like AA6082, are used in the automotive industry for structural components (i.e. body panels) owing to their formability and relatively high strength [1].

The quaternary 7xxx series alloys (Al-Zn-Mg-Cu) possess considerably more strength and would be a prime candidate to increase lightweighting of crash relevant parts in automotive applications. Their widespread application is hindered by a low formability, due to Zn and Mg precipitates, among other things.

Following the thought to find a solution for this hurdle, the concept of Tailor Alloyed Blanks (TAB) can be used to improve the flexibility of the material through local modifications. TAB consists currently of for main technologies [2]. In the first method, Patchwork Blanks (PB), a base plate is reinforced by locally attaching additional plates of varying thicknesses using a welding process. This method offers the advantage of high geometric flexibility combined with high cost efficiency. At the same time, it carries the risk of abrupt stiffness transitions due to the additional plate, which can lead to local stress accumulation, wrinkling and springback during forming processes [3].

In the second method, Tailor Welded Blanks (TWB), several plates with different chemical compositions are joined by welding in order to achieve locally different mechanical properties in a material-efficient manner. However, this approach can lead to highly variable microstructures and unwanted microstructural changes in the joint and heat-affected zone. This can result in a reduction in formability due to local hardening or softening mechanisms and increase the risk of failure during forming [4].

Looking at the third method, Tailor Rolled Blanks (TRB), only a limited effect on formability can be achieved, as it solely involves geometric adjustment in the form of successive thickness reductions by rolling, without modifying the microstructural properties of the material [5].

The fourth method, Tailor Heat Treated Blanks (THTB), uses microstructural changes through local heat-treatments in order to modify mechanical properties. Although, this method can significantly improve formability, it is restricted to heat-treatable alloys and in resolution and complexity due to limited diffusion kinetics [6]. Additionally, THTBs have limited storability, as the effects of heat treatment are time-limited [7].

Similar observations and results were described by Vollertsen et al. [8]. Their work shows that by heat treating plate material with a laser the formability can be increased by dissolution of precipitates. Unfortunately, this process is time sensitive as the heat treatment creates a metastable super saturated solid solution and with enough time precipitation will restart [7].

Avoiding this time-sensitive behaviour can be achieved by adjusting the composition locally in areas that require high formability. To realize this permanent and local change in chemical composition and formability, multiple approaches can be considered, which were described by Stephan et al. [9]. One method could be to reduce the content of the main strengthening elements Zn and Mg using their significantly lower boiling point and higher vapor pressure compared to the other elements [10]. These properties, which can be seen in Table 1 and Figure 1 respectively, allow preferential evaporation during laser welding.

Goal of this work is to use selective element evaporation to adapt the local chemical composition and mechanical properties of AA7075 in preparation of improvement of formability. Therefore, the influence of the process parameters on the evaporation efficiency is analysed. Furthermore, the mechanical properties represented by the material hardness is exemplarily investigated on a representative parameter set.

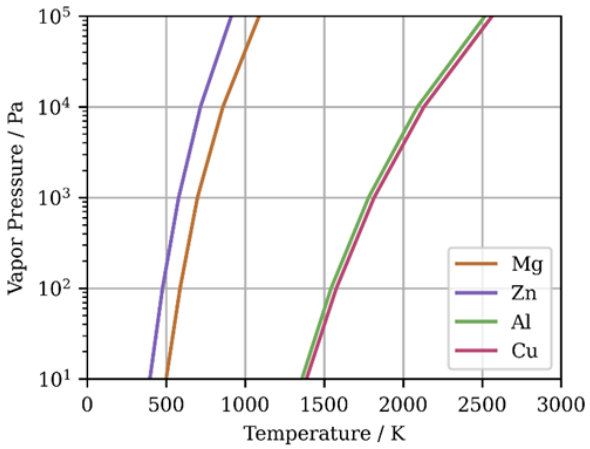

Figure 1: Vapor pressure of main alloying elements of AA7075 [10]

2. Materials and Methods

The plate material was AA7075-F (Novelis Inc.) with the dimensions 50x50x2 mm. The composition according to EN-573-3, as well as composition measured by SEM-EDS is listed in Table 1. Welding was carried out with TRUMPF TruDisk 6001 disk laser and a TRUMPF BEO D70 focusing optic with a beam diameter of 218 µm in focus. In preliminary investigations, relevant parameters and parameter ranges were established. Laser power, velocity, beam size, and the number of times a process was carried out consecutively (hereafter called repeats) were systematically varied within these predefined boundaries using a face-centred central composite response surface design to elucidate their impact on vaporization. Detailed parameter levels are presented in Table 2. The beam size is varied by defocusing the beam.

To accommodate for the different penetration depths all processes were done on five plates clamped on top of each other. The seam length was 30 mm. To analyse elemental loss, cross sections from the middle of the seam were prepared metallographically. This position was chosen to analyse the concentration during steady-state welding, without influences of in- and outcoupling. These samples were analysed with SEM-EDS to determine elemental loss due to vaporization during laser illumination. Each measurement was taken across a 200x200 µm area in up to five places. Three measurements across the width just below the surface (left, centre, right). Another two to three measurements, depending on the weld depth, were taken along the weld centre line (top, middle, bottom). Centre and top correspond to the same measurement.

Table 2. Composition of AA7075 base material according to EN-573-3 and measured by SEM-EDS. Additionally, boiling points of elements are listed [4].

Element	**Al**	**Zn**	**Mg**	**Cu**	**Fe**	**Si**	**Cr**	**Ti**
EN-573-3 [wt.-%]	Bal.	5.1 – 6.1	2.1 – 2.9	1.2 – 2.0	0.5	0.4	0.18 – 0.28	0.2
Measured [wt.-%]	90.5 ± 0.3	5.6 ± 0.2	1.7 ± 0.02	1.6 ± 0.1	0.18 ± 0.02	0.16 ± 0.01	0.22 ± 0.01	0.04 ± 0.01
Boiling Point [°C]	2520	907	1090	2560	2860	3270	2672	3285

The EDX data was used to develop a statistical model to illustrate the influence of process parameters on the evaporation. A 95% level of significance was chosen, meaning factors or interactions with a p-value greater than 0.05 were considered statistically insignificant. Additionally, a hierarchy rule was applied which eliminates factors or interactions starting with the most complex ones. Laser power possessed a p-value of 0.065, yet due to it being a major process parameter, it was decided to not eliminate the factor.

Table 1. Process parameter levels for design of experiment study.

Levels	**-1**	**0**	**+1**
Laser Power [kW]	1.0	1.5	2.0
Welding Speed [mm/s]	5.0	15.0	25.0
Beam Size [µm]	218	317	509
Repeats [-]	1	2	3

3. Results and Discussion

Fig. 2 depicts the average concentrations across the entire melt pool. Our experiments demonstrate a potential loss of Zn of up to 82% and for Mg of up to 78%. The data shows a strong linear relationship (R^2 = 0.97). Differences in relative maximum elemental loss could be due to the lower boiling point and higher vapor pressure of Zn.

The measured concentration of Zn and Mg in the plate material used in these experiments is shown as a grey line, whereas the light red shaded areas show the composition range according to DIN EN-573-3 [11]. While the measured Zn content is within this range, the Mg concentration is lower. Furthermore, many of the welds exhibit higher Mg concentrations than those measured in the base material, possibly because of local concentration gradients due to the intrinsic heat treatment during welding.

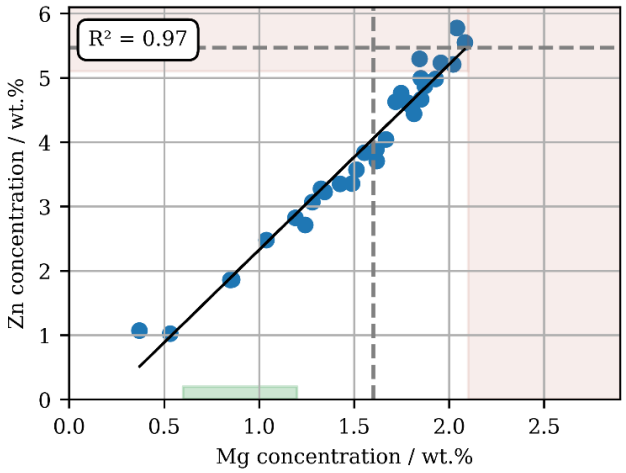

Figure 2: Zn and Mg concentration of analysed welds with linear regression fit (black line) and corresponding R2 value. The area shaded in red displays the concentration ranges of Zn and Mg according to EN-573-3, whereas the green area shows the concentration range for AA6082. The grey dotted line displays the measured concentration of the base metal.

The green shaded area displays the targeted concentration range for Zn and Mg for AA6082 as a reference. While the Mg concentration can meet these requirements, the Zn content is still too high.

3.1. Parametric influence on evaporation

To further optimize this process a regression model was developed to determine the importance of the parameters and main effects on the total volatile element concentration (*TVEC*). With an R^2 value of 76,02%, this model was able to correctly predict the concentration of several welds during validation. Therefore, the model is well suited to predict the influence of the process parameters on *TVEC.*

The pareto plot in Fig. 3 shows how strong the parameters influence the output variable *TVEC*. Beam size is the most important factor, followed by welding velocity and number of repeats. Laser power appears to only have a small influence.

The main effect plot in Fig. 4 shows the directionality of the effects on *TVEC*. Vaporization increases with beam size. This agrees well with results from Jandaghi et al. [12], who argue that a higher surface-to-volume ratio, wherein the surface area acts as a sink and the melt pool volume as a source of Zn and Mg atoms, leads to more evaporation. The importance of the surface area can be explained by the necessity of a liquid-gas interface for evaporation and the fast process times during laser welding, which reduce the significance of mass transfer to the interface by diffusion or convection. Furthermore, a bigger beam leads to improved outgassing behaviour [13].

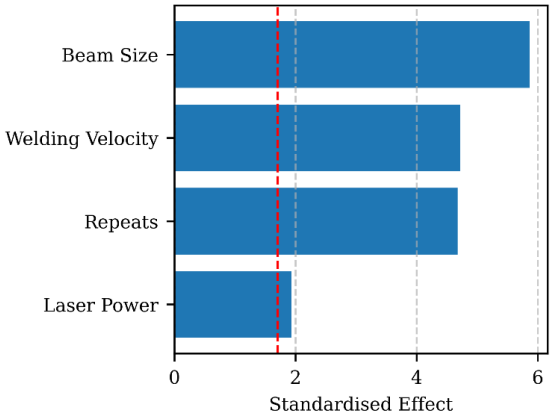

Figure 3: Pareto plot of standardized effects for the statistically relevant parameters.

Additionally, vaporization increases with lower welding velocities and more repeats of the weld. Both factors increase the process time above the boiling point of Zn and Mg [14].

In these experiments the concentration of volatile elements decreases with lower laser power, which disagrees with earlier authors [12, 15]. Jandaghi et al. [12] argue, that higher laser power increases welding depth and surface area, the latter to a stronger degree. This would be beneficial for a higher evaporation rate. One likely explanation for this behaviour is that welding in the chosen parameter set is very unstable, generating large amounts of spatter, which will lead to loss of cross-sectional area in the weld. Spatter generation most likely takes place in the wake of laser beam, thus moving the liquid-gas interface lower into the weld. These areas are expected to be at lower temperatures and vapor pressures. The new interface trails the laser beam and won't be directly irradiated, therefore not reaching the temperatures of the original surface layer. This behaviour could also potentially explain the low statistical significance of the parameter in the regression.

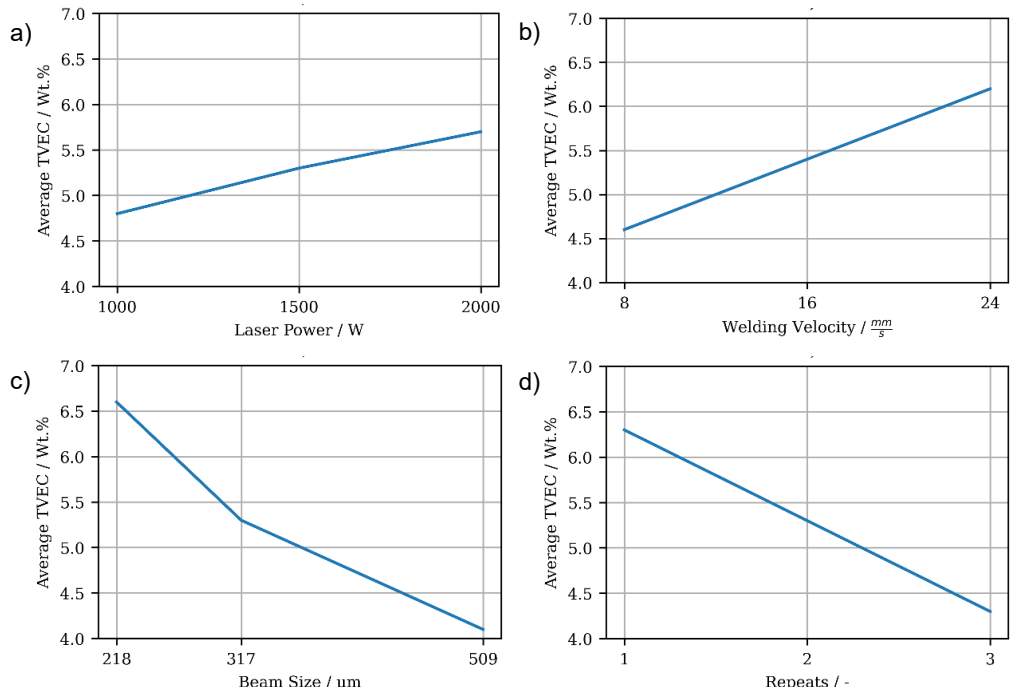

Figure 4: Main Effects plot for a) Laser Power, b) Welding Velocity, c) Beam Size, d) Repeats.

3.2. Concentration gradients in the seam

Isotropic mechanical properties, necessary for widespread application in industry, require a homogenous concentration profile across the width and depth direction. To investigate if gradients exist in the welds all measurements were plotted as boxplots grouped by their position in Fig. 5 and compared across multiple parameters with a non-normally distributed data set. Therefore, the median was used for this analysis.

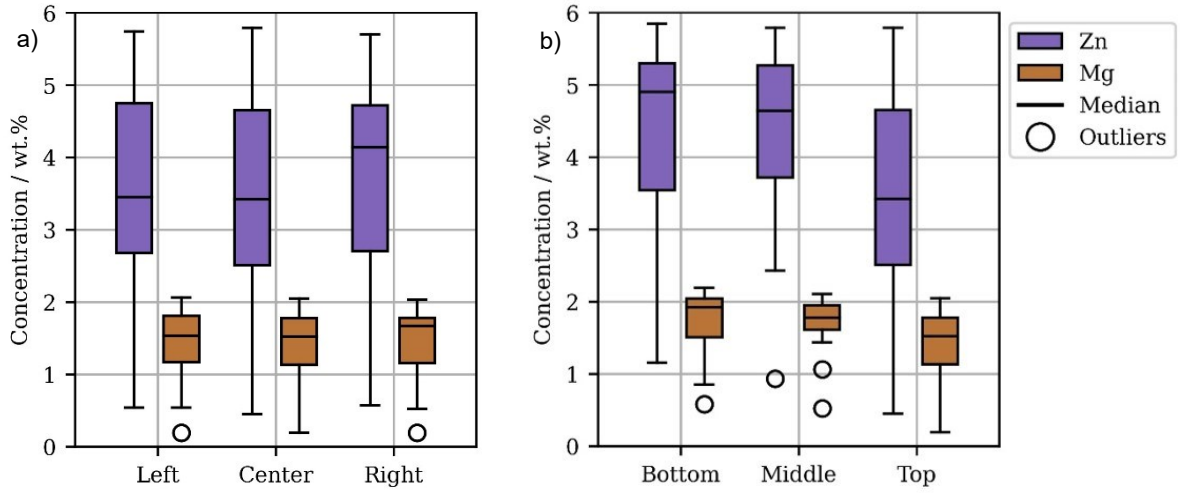

Figure 5: Boxplot of the concentrations for both Zn and Mg grouped by their position in the weld for (a) the width direction and (b) the depth direction.

The concentration profile in width direction is shown in Fig. 5a). The differences are small with concentrations ranging from 3.45 wt.% and 3.42 wt.% to 4.14 wt.% for Zn and 1.53 wt.%, 1.52 wt.% to 1.67 wt.% for Mg from left to right, respectively. The lowest median concentration is achieved in the centre with slightly higher concentrations on the left side,

whereas the right shows the highest values by a significant margin. The intensity distribution of the gaussian beam is expected to lead to the highest temperatures in the weld centre and lower temperatures in the shoulders, which would explain the comparatively higher concentrations on the sides. The difference on the left side is very small compared to the right side which cannot be explained based on the intensity and heat distribution in the process zone.

The boxplot of the concentrations in depth direction is plotted in Fig. 5b. The lowest median concentration with 3.42 wt.% for Zn and 1.52 wt.% for Mg is achieved just below the surface and then increases with welding depth to 4.65 wt.% and 4.90 wt.% for Zn and 1.78 wt.% and 1.92 wt.% for Mg.

This concentration gradient most likely appears due to inhomogeneous temperature distribution in the work piece. The highest temperatures will be reached close to the surface, with decreasing temperatures as the weld depth increases. Furthermore, evaporation requires a liquid-gas interface which requires mass transfer to the surface from lower melt pool regions, either by convection or diffusion, which take longer.

3.3. Hardness gradients in the seam

Lastly, hardness measurements have been done on the cross sections of three samples processed with the same parameter set (laser power P_L = 1500 W, velocity v_L = 5 mm/s, beam size d_L = 317 µm and repeats = 2). The hardness curve can be seen in Fig. 6. The cross sections of the middle of the seams were prepared. For each data point three hardness measurement in the horizontal middle of the cross section with a distance of 0.2 mm to each other have been done. Starting just below the surface, the hardness gradient was mapped.

As can be seen in the plot, with increasing depth the differences between the hardness curves of the samples are getting bigger. Sample 1 in particular exhibits significantly lower hardness values than the base material and the other two samples. Nevertheless, when comparing the hardness curves with Fig. 5b, a correlation between Zn and Mg concentration and measured hardness can be seen. A clear trend towards lower hardness and lower element concentration directly below the surface and towards increasing hardness and element concentration with increasing depth can be seen. This can be explained by the hardening effect of Zn and Mg [13]. With lower Zn and Mg concentrations at the surface, the hardening effect and thus the measured hardness decrease accordingly. With increasing depth, the Zn and Mg content rises and the measured hardness increases again.

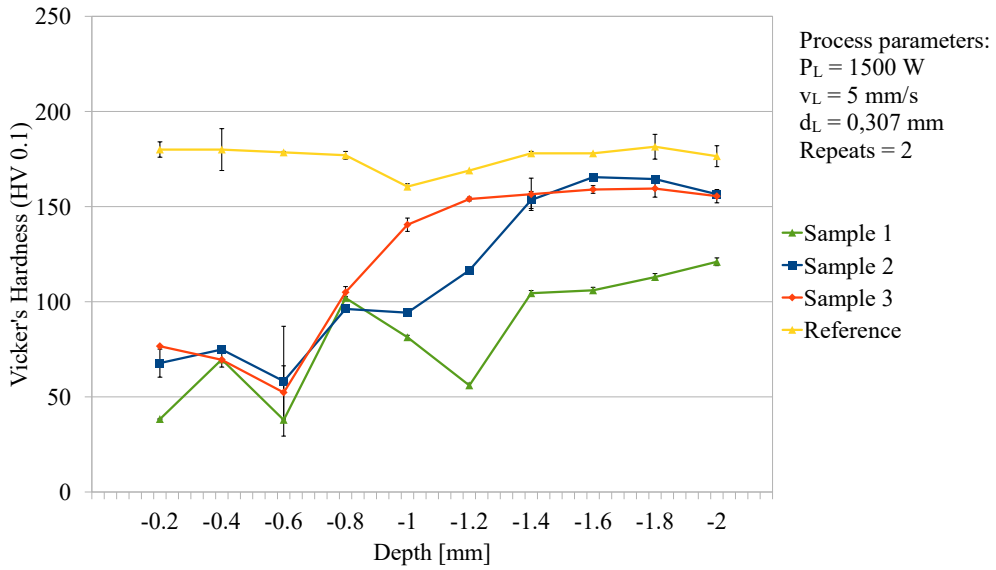

Figure 6: Hardness gradient of base material (reference) and three samples process by the same parameter set (laser power P_L = 1500 W, velocity v_L = 5 mm/s, beam size d_L = 317 µm and repeats = 2) over the depth of the seam.

4. Conclusion and Outlook

In this work the correlation between process strategy and evaporation of volatile elements was studied without consideration of defects and process stability. It could be shown that high elemental loss of up to 82% for Zn and 78% for Mg are feasible. In all cases the Zn content is higher than that of the reference 6xxx series alloy, while only some welds

exhibit Mg concentrations in the desired range. Maximum evaporation can be achieved through high evaporation area and time, which was achieved by a large laser spot size and process time (low welding velocity and multiple repeats). Also, Evaporation is depending on the position in the weld seam. The highest evaporation was achieved in the top. The evaporation efficiency decreased values in depth and width direction due to gradient temperature fields. These concentration gradients are detrimental to isotropic mechanical properties.

Furthermore, local mechanical properties like hardness can be modified using the approach of localized “de-alloying” and selective element evaporation. The hardness correlates with the element concentration of Zn and Mg, as these are the main strengthening elements.

Nevertheless, it could be observed that the process is very unstable with a significant amount of porosity, spatter and macro- and microcracks. Therefore, investigations must be carried out to alleviate these problems and make this process feasible for industry applications. Further analysis of the correlation between Evaporation of volatile elements and local and global mechanical properties, as well as studies on the applicability on area applications, will be performed in the near future.

Acknowledgements

We would like to thank the German Research Foundation (Deutsche Forschungsgemeinschaft, DFG) for funding the research project “Tailor Alloyed Blanks” (project number 521490180). Furthermore, the authors gratefully acknowledge funding of the Erlangen Graduate School in Advanced Optical Technologies (SAOT) by the Bavarian State Ministry for Science and Art.

References

[1] M. Tisza, I. Czinege, Comparative study of the application of steels and aluminium in lightweight production of automotive parts, International Journal of Lightweight Materials and Manufacture 1 (2018) 229–238.
[2] M. Merklein, M. Johannes, M. Lechner, A. Kuppert, A review on tailored blanks—Production, applications and evaluation, Journal of Materials Processing Technology 214 (2014) 151–164.
[3] A review on tailored blanks-Production, applications and evaluation - 1-s2.0-S0924013613002653-main.
[4] M. Krishnamraju, P.V. Reddy, B. Appalanaidu, R. Markendeya, Mechanical behavior and forming characteristics of tailor-welded blanks of structural materials: a review, Multiscale and Multidiscip. Model. Exp. and Des. 7 (2024) 3133–3151.
[5] R. Kopp, C. Wiedner, A. Meyer, Flexibly Rolled Sheet Metal and Its Use in Sheet Metal Forming, AMR 6-8 (2005) 81–92.
[6] M. Geiger, M. Merklein, U. Vogt, Aluminum tailored heat treated blanks, Prod. Eng. Res. Devel. 3 (2009) 401–410.
[7] A. Poznak, D. Freiberg, P. Sanders, Automotive Wrought Aluminium Alloys, in: Fundamentals of Aluminium Metallurgy, Elsevier, 2018, pp. 333–386.
[8] F. Vollertsen, K. Lange, Enhancement of Drawability by Local Heat Treatment, CIRP Annals 47 (1998) 181–184.
[9] M. Stephan, Local adaptation of aluminum blanks through laser de-alloying and wire alloying, in: Sheet Metal 2025, Materials Research Forum LLC, 2025, pp. 365–373.
[10] W.M. Haynes, CRC Handbook of Chemistry and Physics, CRC Press, 2014.
[11] Deutsches Institut für Normung, DIN EN 573-3, Aluminium und Aluminiumlegierungen - chemische Zusammensetzung und Form von Halbzeug. Teil 3, Chemische Zusammensetzung und Erzeugnisformen: = Aluminium and aluminium alloys - chemical composition and form of wrought products. Part 3, Chemical composition and form of products, Deutsche Fassung EN fifthsevenththird-third:twentiethnineteenth + Asecond:twentiethtwenty-third, Beuth Verlag GmbH, Berlin, 2024.
[12] M. Jandaghi, P. Parvin, M.J. Torkamany, J. Sabbaghzadeh, Alloying element losses in pulsed Nd YAG laser welding of stainless steel 316, J. Phys. D: Appl. Phys. 41 (2008) 235503.
[13] J. Enz, S. Riekehr, V. Ventzke, N. Huber, N. Kashaev, Fibre laser welding of high-alloyed Al–Zn–Mg–Cu alloys, Journal of Materials Processing Technology 237 (2016) 155–162.
[14] M.J. Cieslak, P.W. Fuerschbach, On the weldability, composition, and hardness of pulsed and continuous Nd:YAG laser welds in aluminum alloys 6061,5456, and 5086, Metall Trans B 19 (1988) 319–329.
[15] P.A.A. Khan, T. Debroy, Alloying element vaporization and weld pool temperature during laser welding of AISI 202 stainless steel, Metall Trans B 15 (1984) 641–644.